NASA TECHNICAL MEMORANDUM

NASA TM-75788

NASA-TM-75788 19800012799

INVESTIGATIONS REGARDING THE DRAG CHARACTERISTICS OF FLOW-DISTURBING BODIES WHICH ARE ARRANGED IN LINE AND ATTACHED TO THE WALL.

M. Balkowski and H. Schollmeyer

NATIONAL AERONAUTICS AND SPACE ADMINISTRATION
WASHINGTON, DC   20546   MARCH 1980

1. Report No. NASA TM 75788	2. Government Accession No.	3. Recipient's Catalog No.
4. Title and Subtitle Investigations Regarding the Drag Characteristics of Flow-Disturbing Bodies Which Are Arranged in Line and Attached to the Wall.		5. Report Date MARCH 1980
		6. Performing Organization Code
7. Author(s) M. Balkowski and H. Schollmeyer		8. Performing Organization Report No.
		10. Work Unit No.
9. Performing Organization Name and Address SCITRAN Box 5456 Santa Barbara, CA 93108		11. Contract or Grant No. NASw- 3198
		13. Type of Report and Period Covered Translation
12. Sponsoring Agency Name and Address National Aeronautics and Space Administration Washington, D.C. 20546		14. Sponsoring Agency Code

15. Supplementary Notes

Translation of "Untersuchungen zum Widerstandsverhalten hintereinander liegender wandfester Storkorper", Rheinisch-Westtaelische Technische Hochschule, Aerodynamisches Institut, Abhandlungen, no. 21, Dec. 1974, pp 20-24 (A75-23097)

16. Abstract

An investigation was conducted regarding the flow characteristics of rectangular bodies which were mounted on the base area of a rectangular closed wind tunnel. As many as four bodies were mounted in line with equal distances between successive bodies. The Mach number of the flowing air was in the range from 0.1 to 0.5. Total and individual drag values could be changed within a wide range by a suitable selection of the distance between successive bodies.

17. Key Words (Selected by Author(s))	18. Distribution Statement Unclassified - Unlimited	
19. Security Classif. (of this report) Unclassified	20. Security Classif. (of this page) Unclassified	21. No. of Pages 15	22. Price

INVESTIGATIONS REGARDING THE DRAG CHARACTERISTICS OF
FLOW-DISTURBING BODIES WHICH ARE ARRANGED IN LINE AND
ATTACHED TO THE WALL.

M. Balkowski and H. Schollmeyer

I.   Introduction and Problem Formulation

The mutual influencing of perturbation bodies arranged in
a row in a flow field is becoming more and more of practical
importance because of its drag behavior and the corresponding
momentum loss in the flow. Many questions of construction
air dynamics as well as problems in the design of flow systems
for chemical processes, high performance heat exchangers and
filters involve these detailed investigations. Up to the
present only a few papers are known which treat the influence
of perturbing bodies attached to the wall which penetrate beyond
the incident boundary layer [1, 2, 3].

In the following we will discuss the flow behavior of iden-
tical rectangular perturbation bodies which are attached to
a base surface on the wall in a rectangular enclosed flow channel
(Figure 1). Up to four perturbation bodies with the same separa-
tion were installed. The distance between them was varied between
1 to 24 perturbation body heights, and the Mach number of the
incident air was varied between 0.1 and 0.5.

II.   Description of the Flow Behavior

The investigative perturbation bodies make the flow separate
along the sharp edge which faces the flow. In the separation sur-
face which is then created there are large velocity gradients and
therefore large shear forces which lead to the formation of a strong
turbulent mixing zone. The turbulence is for the most part in-
homogeneous and isotropic and has an intermittent character espec-

---

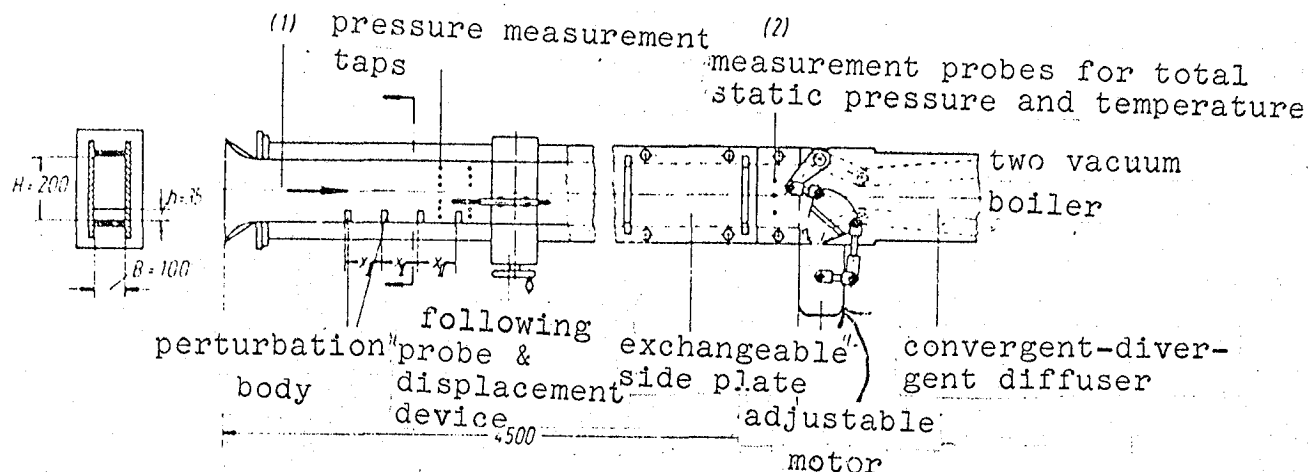*Numbers in margins indicate foreign pagination.

Figure 1. Cross-section (dimensions in mm). /20

$x_{II}/h = 6$ $M_0 = 0.44$
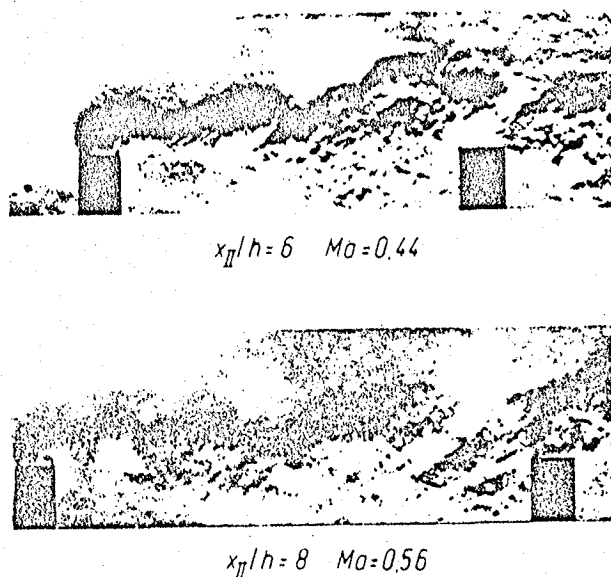

$x_{II}/h = 8$ $M_0 = 0.56$

Figure 2. Schlieren photograph of the flow.

ially at the edge, so that measurements are especially difficult in this region. The Schlieren photographs for two different distances between the first and the second perturbation body (Figure 2) give an impression about the velocity fluctuations which prevail in this case. The drag of the first perturbation body depends almost exclusively on the incident flow conditions. The drag of the following perturbation body passes through two characteristic stages as the separation is increased: if the perturbation body is in the region of the dead water region (Figure 3 above), then the
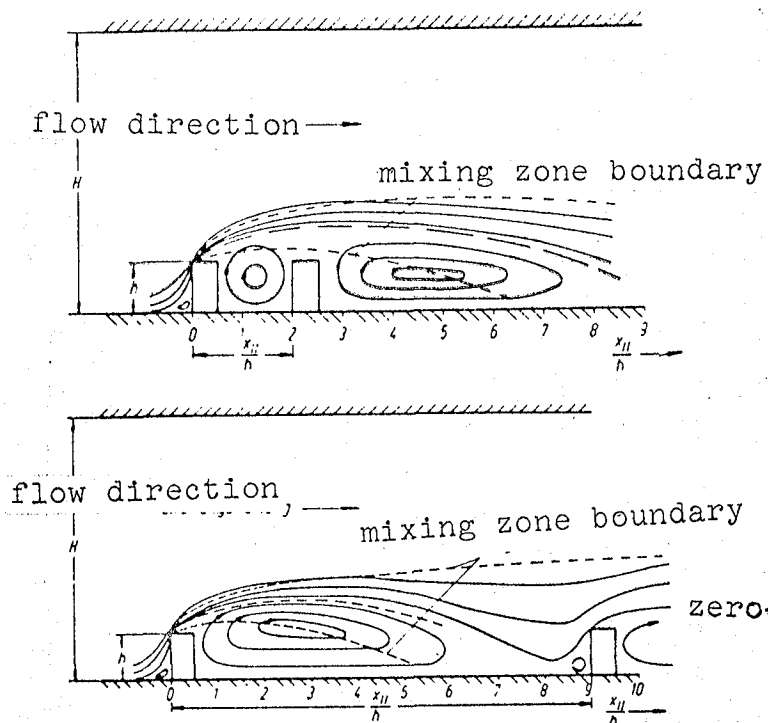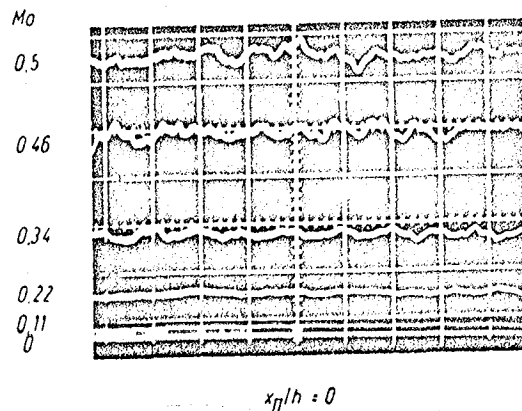
2

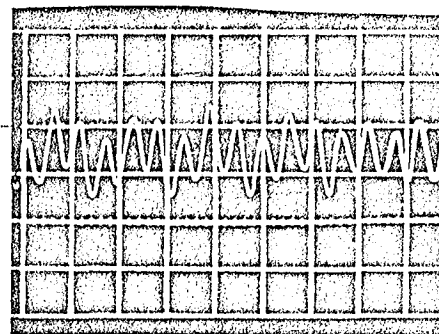Figure 3. Streamline configuration of the perturbation body wake; top for a small separation and on the bottom for a large separation.
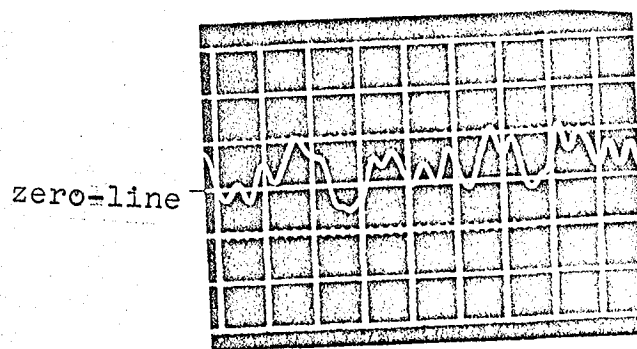

$x_{II}/h = 0$

Time deflection: 2ms/cm
Sensitivity: 2.25 kp/cm

$x_I/h = 4$ $M_0 = 0.5$

Time deflection: 1 ms/cm
Sensitivity: 4.5 kp/cm

$x_{II}/h = 8$ $M_0 = 0.5$

Time deflection: 1 ms/cm
Sensitivity: 4.5 kp/cm

Figure 4. Drag fluctuations for different load cases.

drag is negative. The force on the front side and the back side
is determined essentially by the corresponding static pressure of
the flow above the mixing zone. As the separation is increased
the perturbation body becomes more and more under the influence of
the mixing zone (Figure 3, bottom). The drag becomes positive
and increases further with increasing incident flow speed.   /21

III. Test Configuration and Measurement Methods

1. Test Configuration

The measurements were performed in a 450 cm long "Suction
Channel" with a rectangular cross section (H = 200 mm, b = 100 mm)
(Figure 1). The walls consisted of "high impact polyvinylchloride"
(Hostalit Z^R), a plastic 2cm thick. A convergent-divergent dif-
fusor which comes after these walls provided a capability for adjust-
ment and for holding the velocity constant. The height and position
of the perturbation bodies was determined from the following con-
sideration:

a) The first perturbing body is to clearly penetrate above
   the boundary layer which is between 4 to 7 mm thick.

b) The aperture ratio $(H-h)/H$ for an incident Mach-number
   of $Ma \lesssim 0.1$ allows one to expect a constant flux coef-
   ficient over the Re number formed with the free opening
   dimension $(H-h)$. According to DIN 1952 [5], this
   leads to $h/H \lesssim 0.2$. When the channel height H is
   enlarged, the contraction and shape of the flow remain
   independent of the Re number referred to the incident
   flow speed.

2. Pressure measurement

The rest pressure was measured using a Pitot tube, and the
static pressure was measured using a large number of pressure
taps (diameter 1 mm) in the side walls of the channel.

4

A measurement point switch (Scanivalve) was used to acquire and print out the values at 48 measurement points, using a transducer (CEC) and an associated measurement and control facility. This occurred during the blowing time of the channel of about 20 seconds.

We only use measurements in the non-turbulent flow region above the mixing zone for the evaluation, because detailed investigations [4] show that the strong velocity fluctuations in the perturbing body wake do not allow one to obtain a reliable evaluation of the flow field using pressure measurements.

3. Force measurement

We also have to be skeptical about determining the perturbation drag with pressure distribution measurements in experiments, because the influence of the turbulent fluctuations on the measured pressure can only be determined in an uncertain way. Tests/22 along these lines were not successful. Only measurements of the force Kn applied to the perturbing body in the main flow direction (x) with an installed strain measurement balance, which was dynamically matched to the fluctuating loads, led to the reproducible results.

Figure 4 shows the force applied to the perturbing body by the flow as a function of time. As to be expected, the first Mach numbers which were used for all cases show a uniform load as was expected (top photograph). A second perturbing body in the dead water region shows the greatest load fluctuations for a separation ratio of $x_n/h = 4$, and the average value is negative (central figure). With increasing distance the fluctuations decay again and the average value again becomes positive (lower figure). When comparing the oscillograms, one has to consider the different input sensitivities of the measurement amplifiers.

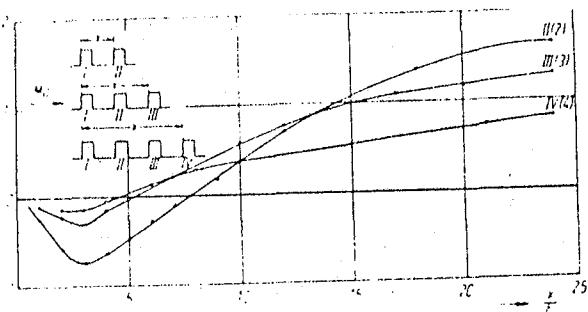The temperature-compensated strain balance was switched as

Figure 5.   Drag coefficient of the last perturbation in each
            case for different groups at $Ma \approx 0.35$

the load branch of a Wheatstone full bridge.   It allows one to
accurately and simply determine the forces in the x-direction
with a high resolution in time (eigen frequency $\approx 2500\ Hz$) and
the interference is small ($K_y/K_x < 0.02$), i.e., a force K_y
perpendicular to the main flow direction leads to a measurement
error in the x-direction of less than 2% of this force.

     Because of the strong fluctuations the data were acquired
with a true integrating analog-digital measurement system.   The
force measured in this way was made dimensionless using the
area projected in the flow direction $F_{st} = b \cdot h$ and the stagnat-
ion pressure $\varrho \cdot w^2/2$.

     4.   Measurement of the Momentum Loss

     The momentum loss was determined by measuring pressure and
velocity ahead of (1) and far behind (2) the perturbing bodies.
It is the result of the drag of the bodies and the friction force
which corresponds to the friction losses at the channel wall, as
well as on the perturbing body configuration.   This friction force
can also not be determined.   However the friction force of the
empty channel can be determined as

$$K_{Reibu, L} = F_K \left[p_1 - p_2 \right]_L - \varrho_1 w_{1L} \left(w_2 - w_{1L} \right)$$

The energy loss with the installed perturbing bodies is the result
of the drag of all of the perturbing bodies K_{st} and the friction

6

resistance at the channel walls $K_{Reibg\,L} + \sqrt{}\,K_{Reibg}$ in relation
to the empty test section. The momentum theorem is therefore:

$$K_{St} + K_{Reibg\,L} + \Delta K_{Reibg} = F_K \left[(p_1 - p_2)_M - \varrho_1 u_1^2{}_M - u_1^2{}_M \right]$$

If the measured values p and w are referred to the same throughput
$\varrho_1 w_{1L} \quad \varrho_1 w_{1M}$, then the drag which is equivalent to the total
momentum is

$$K_{St} + \Delta K_{Reibg} = F_K \left[(p_{2L} - p_{2M}) + \varrho_1 u_1^2 (u_{2L}^2 - u_{2M}^2) \right]$$

and the corresponding loss coefficient is

$$c_w = 2 \left(\frac{p_{2L} - p_2}{\varrho_1 w_1^2} M + \frac{w_{2L} - w_{2M}}{w_1} \right) \frac{F_K}{F_{St}}$$

Measurements not reproduced here show that the change in the
wall friction force is of the same order as the perturbation body
drag.

Since the wall friction force cannot be determined or ignored
it is not possible to determine the force applied to the perturbing
bodies using measurement of the momentum loss in the present case.

IV. Results

1. Drag Behavior

The drag variation of the individual perturbing bodies in
a group of several perturbing bodies arranged in a row behind one
another allows one to establish 3 influencing variables: the
position i $(i = $ I, II, III. . . ., $n)$, the separation ratio (x/h) and the
incident Mach number Ma:

$$c_w = c_w (i, \tfrac{x}{h}, Ma)$$

Figure 5 shows the drag coefficient of the last perturbing body
of a group of 2, 3 and 4 for Ma 0,35 . With increasing posi-
tion number the characteristic feature, negative coefficient in

7

the dead water region, increase for increasing separation, is maintained. The drag as a distinct minimum for all positions at $x/h \approx 3$. With increasing separation the perturbing body comes more and more under the influence of the high incident flow speed, and its drag asymptotically approaches the drag which it would have if it were the first body, but for different flow conditions.

Changes in the flow field and the drag become smaller with increasing position number, so that an increase in the number of disturbing bodies for technically feasible separations $(x/h > 5)$ leads to a decreasing change in the total momentum flux as Naumann [1] already established. An explanation for this was given by Kauder [6] who observed that, because of the transport of kinetic energy perpendicular to the flow direction caused by the large turbulence in the perturbing body wake, already after a few perturbing bodies a turbulent velocity profile occurs in the test section, which then no longer changes downstream. The non-turbulent flow above the mixing zone is displaced by   /23 the perturbing bodies in such a way that perturbing bodies with the higher position numbers (>5) contribute an additional loss in mechanical energy only to the extent as is required for maintaining the strong boundary layers.

Therefore we can expect that the detailed investigation of a group of four, discussed in the following, will also be representative for larger numbers of perturbing bodies (Figure 6). The drag coefficient of the individual perturbing bodies was plotted in this representation over a common separation variable

$$\frac{x''}{h} = \frac{x'}{h} = \frac{1}{2}\frac{x''}{h} = \frac{1}{3}\frac{x'''}{h} \qquad i=i\ \frac{x_i}{h}$$

for all disturbing bodies, so that the corresponding c_w-values lay above one another in the ordinate direction.

The drag coefficient of the first perturbing body I (4) is for the most part independent of the Ma number and the dis-
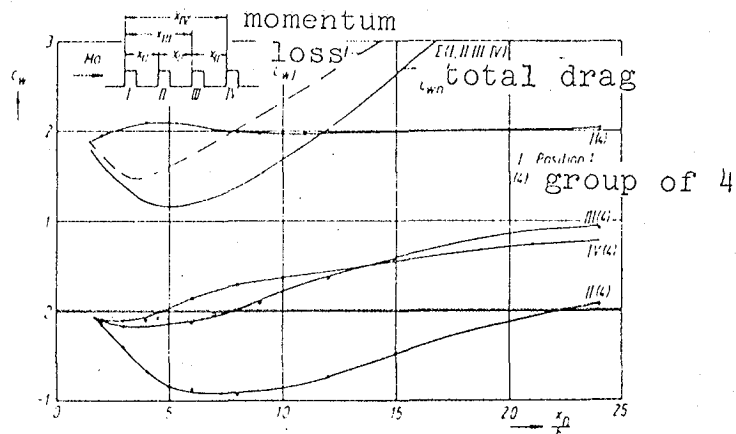
8

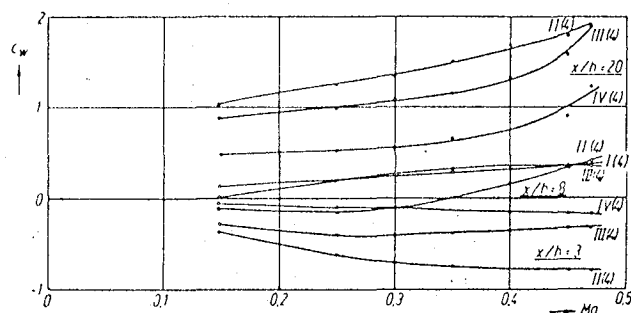Figure 6. Drag coefficients of a group of four at $Ma \approx 0.35$.

Figure 7. Drag coefficients of the individual perturbation bodies of a group of four.

tance ratio at C_W equals 2. It is only at $x_n/h < 7$ that the perturbation of the recirculation region leads to substantial deviations. The drag of the following perturbing bodies shows the typical behavior already given in Figure 5.

If one considers the different abscissa units in the form $(i-1)x_n/h \quad x_i/h$, then the internal perturbing bodies in the configuration of II (4) and III (4) only show slight differences in their behavior compared with the groups of two and three. The flow field downstream of each perturbing body has no noticeable influence on its drag as already established for the first perturbing body.

The total drag of this group of four can be determined as the sum of the individual drag values as a function of a common distance variable x_n/h .

$$c_w = \sum_{i=1}^{4} c_{wi} \left(\frac{x_{11}}{h} \right)$$

It results from this that a system of four perturbing bodies will have a substantially reduced drag coefficient compared with a single perturbing body having the same dimensions, up to a distance ratio of $x_{11}/h = 11$. For $x_{11}/h = 5$ the drag reduction is 40%. This means that if additional perturbing bodies of the same kind are installed in the vicinity of a perturbing body, the total drag decreases. This means that additional internal stiffening members of a flow wind tunnel or the division of an individual reinforcement member into a number of smaller parts of the same strength has a favorable effect on the drag and the flow direction, if certain geometric conditions are maintained.

The influence of the Ma number on the drag coefficient of the perturbing bodies II, III and IV in the group of four is shown in Figure 5 for the distance ratios $x_{11}/h = 3; 8$ and 20. The incident Mach number was increased until the supersonic region created above the perturbing bodies no longer allowed any increase. The representation shows that the characteristic feature of the drag behavior with increasing Mach number becomes more pronounced, independent of whether there is a positive or negative drag coefficient. At $x/h = 8$ the drag coefficient of the second body changes sign; because of increasing Mach number the mixing zone moves toward the dead water condition and these perturbing bodies then enter the region of the core flow more and more.

2. Momentum loss

In addition to measuring forces we also determine the change in the total momentum flux by measuring the static pressure formed behind the perturbing bodies and by ignoring heat exchange. The
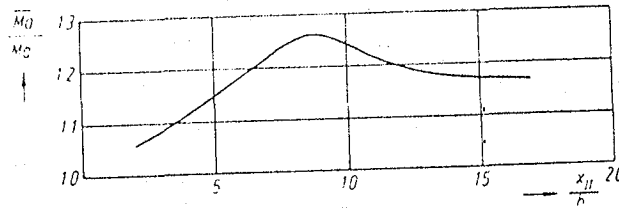
10

Figure 8. Change of the Mach number average value

losses in the empty test section, which amount to about 1/3 of
the total losses, were determined beforehand and were subtracted,
referred to the incident Mach number at point (1).

Figure 6 shows that the momentum loss coefficient c_{wJ}
is greater than the drag coefficient c_{wn}. This was to be ex-
pected according to the design III.4, because in the region of
the perturbing bodies one has to expect considerably higher speeds
than the incident flow speed and therefore higher wall friction
losses $K_{Reibg.1} + \setminus K_{Reibg.}$. In order to determine these fric-/24
tion losses, one has to know the changed velocity field with respect
to measurements in the empty tunnel. This cannot be done without
a high amount of complexity. Therefore a comparison of the two
coefficients has to be restricted to the statement that they are
for the most part similar. The momentum loss is a measure for the
total drag, in a somewhat weaker form because of the additional
friction losses. From the difference $c_{wn}-c_{wJ}$ of Figure 7 we
can obtain information about the magnitude of the velocity in-
creases which are produced by each perturbing body configuration.
Figure 8 for example shows by how much the loss Mach number Ma
must be increased when determining the channel losses of the empty
test section in order to arrive at the same drag coefficient.
This new Mach number $\overline{Ma}$ can be interpreted as the Mach
number average between the measurement planes ahead of (1) and
far behind (2) of the perturbing bodies. It is a measure for the
length of the region of the test section in which there is a sub-
stantially higher speed.

This region is small for small perturbing body separation

11

$(x_n/h < 3)$. It increases until the perturbing bodies and the recirculation regions are immediately adjacent to one another and therefore continuously displace the flow above the mixing zone ($x_n/h = 9$). When the bodies move even closer together, it is divided because of partial reattachement of the boundary layer in individual regions, in which the zones of relatively high speed are relatively short.

V. Final Remarks

The investigations gave us an idea of the difficulties in a detailed evaluation of this interesting flow problem. Using different perturbing body geometries and associations, as other tests not recorded here have shown, there is a possibility of influencing the flow behavior even more. However we do not expect really substantial quantitative changes in the statements given here.

We may summarize the drag behavior of rigidly attached perturbing bodies attached to the wall lying in a row as follows:

1. By suitably selecting the separation, the individual drag and the total drag can be varied over wide limits. In the present case, for example, the drag coefficient of the second body varies within the range $-0,8 \le c_w \le 2$. The variation range for four perturbing bodies was $1,2 \le c_w \le 7$. The minimum was therefore 40% below the c_W – value of an individual perturbing body.

2. Accordingly the loss in mechanical energy of a medium for a given set of perturbing bodies can be influenced over a wide range with a suitable selection of the distance ratios. The corresponding loss coefficient for the four body configurations was between $1,5 \le c_{wJ} \le 7$. The energy savings compared with the configuration with only a single perturbing body was more than 25% in spite of the higher wall friction losses.

VI. References

1. Naumann A., Tests With Air Dynamic Throbbling Systems, ZFW Vol. 9 (1961) p. 117-124.

2. Hoerner, S. F., Interference Drag. Fluid Dynamic Drag, Selbstverlag (1958), Chapter 8.

3. Zeller, H. Muller, A. and Neumann K. D., Investigations of the Flow Behavior in Electro filters. Z "Staub Reinhaltung der Luft" Vol 29 (1969) p. 303-307.

4. Schollmeyer, H., Investigations of a Compressible Turbulent Shear Flow Behind a Dead Water Region, Diss. TH Aachen 1973.

5. VDI Flux Measurement Rules. 1952, Beuth-Vertrieb Koln (May 1969) p. 34.

6. Kauder, K, The flow resistance in wavy tubes. A contribution to the roughness problem. Z "Konstruktion im Masch. - Apparate- and Geratebau" Vol 24 (1972) p. 169-174.